

Surface and bulk properties of hot-pressed PbMo_6S_8 superconductor studied by Auger electron spectroscopy and calorimetry

SELVAM, Parasuraman, *et al.*

Abstract

A direct observation of the grain-boundary phases for several well-characterized hot-pressed PbMo_6S_8 samples were made by Auger electron spectroscopy. The surface elemental concentrations are completely different when compared to its bulk composition. The thickness of this altered composition is in the range 100–200 Å gradually increasing with increase in hotpressing temperature. Also, evidence of segregation of impurities, such as carbon and SiO_2 to the grain-boundaries were noticed for some of the samples. Calorimetric experiments show a continuous broadening and a reduction in amplitude of the specific heat anomaly at T_c . This in terms of superconducting volume fraction indicates a T_c distribution in the range 9–15 K. Such an observation can be related to the local inhomogeneities with respect to the ternary composition, i.e., a deviation from ideal stoichiometry, PbMo_6S_8 . The results are discussed in conjunction with X-ray diffraction, scanning electron microscope, and energy dispersive X-ray analysis. By considering the grain-boundary phases and the calorimetric observation of inhomogeneities, a [...]

Reference

SELVAM, Parasuraman, *et al.* Surface and bulk properties of hot-pressed PbMo_6S_8 superconductor studied by Auger electron spectroscopy and calorimetry. *Applied Physics A: Materials Science and Processing*, 1995, vol. 60, no. 5, p. 459-465

DOI : 10.1007/BF01538770

Available at:

<http://archive-ouverte.unige.ch/unige:114643>

Disclaimer: layout of this document may differ from the published version.



UNIVERSITÉ
DE GENÈVE

Surface and bulk properties of hot-pressed PbMo_6S_8 superconductor studied by Auger electron spectroscopy and calorimetry

P. Selvam¹, J. Cors², M. Decroux², Ø. Fischer²

¹ Department of Chemistry, Indian Institute of Technology, Powai, Bombay 400 076, India
 (Fax: + 91-22/578 34 80)

² Department de Physique de la Matière Condensée, Université de Genève, 24, Quai E. Ansermet, CH-1211 Genève 4, Switzerland
 (Fax: + 41-22/781 21 92)

Received: 27 June 1994/Accepted: 6 January 1995

Abstract. A direct observation of the grain-boundary phases for several well-characterized hot-pressed PbMo_6S_8 samples were made by Auger electron spectroscopy. The surface elemental concentrations are completely different when compared to its bulk composition. The thickness of this altered composition is in the range 100–200 Å gradually increasing with increase in hot-pressing temperature. Also, evidence of segregation of impurities, such as carbon and SiO_x , to the grain-boundaries were noticed for some of the samples. Calorimetric experiments show a continuous broadening and a reduction in amplitude of the specific heat anomaly at T_C . This in terms of superconducting volume fraction indicates a T_C distribution in the range 9–15 K. Such an observation can be related to the local inhomogeneities with respect to the ternary composition, i.e., a deviation from ideal stoichiometry, PbMo_6S_8 . The results are discussed in conjunction with X-ray diffraction, scanning electron microscope, and energy dispersive X-ray analysis. By considering the grain-boundary phases and the calorimetric observation of inhomogeneities, a plausible explanation is given for the low critical current densities in these materials.

PACS: 74.60. – w; 74.60.Mj; 74.70. – b; 74.70.Fi

Ternary PbMo_6S_8 is considered to be one of the promising materials for high-field magnetic applications. It has been studied extensively since the discovery of its high upper critical field ($B_{c2} \sim 60$ T) [1, 2]. The need for bulk materials with higher critical current density, J_C , at fields in excess of those previously measured, has attracted new interest and several investigations have exclusively been devoted to their improvement [3]. Nevertheless, at present, the observed J_C values for the bulk samples are lower by at least an order of magnitude than those of the individual grains or those measured on wires and films [1, 3]. On the other hand, the marginal values exhibited by bulk samples have been thought to be associated with the following facts: (i) Synthesis conditions with respect to

material purity, homogeneity, stability and microstructure. This, however, can easily be avoided by adopting optimized experimental conditions and by using high purity starting materials and stringent measures to prevent contamination during both preparation and processing procedures [4, 5]; (ii) intragrain characteristics like structural disorder, phase transitions, and defects. The occurrence of a structural phase transition [6–8] at low temperature could degrade J_C . Such a transition appears to be suppressed to a considerable extent by alloying [6, 7]; (iii) intergrain weak-link behavior caused by impurity and secondary phases, poor intergrain connections, microcracks and/or non-stoichiometry at the interface. In fact, in the past not much work has been done in this direction.

From a practical viewpoint, the grain-boundary layers and the interconnectivity of the grains are important and may constitute the reason for the low J_C 's obtained so far in the bulk conductors. The various physical measurements performed have failed to confirm the nature and the influence of the grain-boundary phases on the superconducting properties primarily due the lack of a suitable approach. Thus, we have decided to perform Auger Electron Spectroscopic (AES) and calorimetric experiments on these samples. The purpose of this study is also to present surface analysis data for PbMo_6S_8 at different hot-pressing temperatures and to show how it induces an alteration with respect to the ternary composition, resulting in an extended inhomogeneity in the near-surface regions. Preliminary results were presented elsewhere [9].

1 Experimental procedures

1.1 Materials preparation and characterization

PbMo_6S_8 powders were prepared by three different methods [4, 5, 10]. The experimental details are briefly summarized in Table 1 along with certain physical characteristics. Note that two different reaction temperatures, namely 1180 and 1600 °C, were employed for the samples prepared by method I. Unless otherwise stated, the samples used in this investigation were those prepared at

Table 1. Experimental conditions for the preparation of PbMo_6S_8 samples. For comparison, some of their properties are included. All the samples were hot-pressed at 1200°C

| Method | Matrix | Starting materials | Reaction temp. [$^\circ\text{C}$] | Density [%] | Grain size [μm] | Lattice constant ratio, c/a | T_C [K] | RRR ^a | J_C at 4.2 K, 9 T [$\times 10^8 \text{ Am}^{-2}$] |
|--------|------------------------|-----------------------------|-------------------------------------|-------------|------------------------------|-------------------------------|-----------|------------------|---|
| I | Molybdenum crucible | Pb, Mo_6S_8 | 1180 | 95–99 | 0.5–2.0 | 1.2491(1) | 14.80 | 3.8 | 1.8–2.2 |
| | | | 1600 | 88–94 | 5.0–10.0 | 1.2494(1) | 14.75 | 3.8 | 1.4–1.6 |
| II | Boron-nitride crucible | Pb, Mo_6S_8 | 1600 | 85–92 | 5.0–10.0 | 1.2495(1) | 14.80 | 3.8 | 0.4–0.9 |
| III | Quartz tube | Pb, Mo_6S_8 | 1450 | 80–90 | 5.0–10.0 | 1.2435(1) | 11.65 | 2.0 | 0.08–0.5 |

^aResidual Resistivity Ratio—the ratio of the resistivity at room temperature and the resistivity just above T_C

1180°C . To avoid contamination, powder samples were manipulated in an argon-filled glove box. Dense bulk samples were made by hot-pressing the powder samples at 1200°C as per the details outlined previously [5]. In addition, one of the samples produced by method I was hot-pressed at different temperatures in the range 1000 – 1400°C .

All the samples were analyzed by powder X-Ray Diffraction (XRD) technique (Philips automated diffractometer, PW-1710 with a vertical goniometer). The samples were highly crystalline and the peaks were indexed on the basis of hexagonal unit cell. The lattice constants were determined by using silicon as the internal standard. The computed values show consistently high c/a ratio (Table 1), a factor which possibly governs the phase purity with respect to a plausible oxygen contamination. The lower c/a values in the case of samples prepared by method III, are due to a contribution from oxygen substitution in the lattice, $\text{PbMo}_6\text{S}_8-x\text{O}_x$ [4].

The T_C of the samples was measured inductively with different ac-field amplitudes typically at 0.6 – $60 \mu\text{T}$ and a frequency of 87 Hz . The transitions are generally sharp with the exception of one of the samples hot-pressed at 1000°C which showed a broad transition characteristic of granularity [11]. The resistivity was determined by the four-probe method with a frequency of 87 Hz . All of them show sharp resistive transition with a typical width of 0.2 K . The inductive flux profile measurement J_C was carried out by the method proposed by Rollins et al. [12]. The results indicate that the J_C values are primarily dependent on the intergrain connections and the phase purity with respect to the composition [4, 13].

Microstructure analysis was performed on air-fractured samples in a Cambridge instruments (Stereoscan 360) high-resolution Scanning Electron Microscope (SEM) coupled with Energy Dispersive X-ray (EDX) analysis (Tracor Northern, Series II) system. The micrographs indicate that the grain size is strongly influenced by the preparation and processing conditions. EDX analysis revealed the presence of silicon in the oxygen-contaminated phase. Density measurements were carried out with a picnometer using alcohol as the fluid. As expected, the density varies with the processing temperatures (Table 1) which in turn has a direct correlation with the porosity and morphology.

1.2 Auger electron spectroscopy

AES measurements were performed in a VG instruments ESCALAB Mark I spectrometer equipped with SEM, scanning Auger microscopy, quadrupole mass spectrometer and Ar^+ sputtering facilities. The PbMo_6S_8 samples were broken in situ in the analysis chamber with a base pressure of $3 \times 10^{-11} \text{ mbar}$. The system contains a separate preparation chamber, with a base pressure of $1 \times 10^{-10} \text{ mbar}$, where the Ar^+ facility is installed. The energy analyser is a 150° spherical sector type. The samples were sputter cleaned by Ar^+ bombardment at $2 \times 10^{-6} \text{ mbar}$ pressure with a primary beam current of 5 kV and a ion beam current density of $400 \mu\text{A cm}^{-2}$. The spectra reported here (50 – 550 eV) were obtained using a primary beam energy of 10 kV with a primary electron beam current of 200 nA and a modulation energy of 5 V (peak-to-peak amplitude). Selected characteristic transitions, such as sulfur (*LMM*; 155 eV), molybdenum (*MNN*; 190 eV), lead (*NOO*; 92 eV), carbon (*KLL*; 270 eV) and oxygen (*KLL*; 510 eV) were used to follow the changes in surface concentrations. The surface elemental compositions were quantified from the signal amplitudes using standard Auger elemental sensitivity factors [14].

1.3 Calorimetry

Absolute values of the specific heat were obtained by means of a thermal relaxation technique [15]. All the samples exhibit a well-defined specific heat jump at T_C with a transition widths of 0.4 – 0.8 K [4, 5, 10]. The T_C distribution in the sample was obtained by a careful analysis of the electronic specific heat [16]. The findings are significant and important with respect to the improvement of the sample quality.

2 Results and discussion

Both fractured and sputtered surfaces of PbMo_6S_8 show significant differences in the surface and bulk compositions. The former is rich in sulfur and deficient in molybdenum as compared to the latter. This could be attributed to the presence of sulfur-excess binary phases, such as

MoS₂ and/or Mo₂S₃ at the interface. At some grain-boundaries, the sulfur enrichment is high enough to suggest that the near boundary phase consists of PbS, as observed by a simultaneous enrichment of lead on the fractured samples [4, 5]. It is also evident that the Ar⁺ bombardment causes a drastic change in the relative peak intensities of sulfur and molybdenum. Such an effect on a compound material is quite understandable in view of the fact that the masses of elemental sulfur and argon are closely matched, while those of molybdenum and argon are very different. Even more important is that the sputtering yield of molybdenum appears to depend strongly on the chemical environment [17].

Surprisingly, the samples prepared by method III show prominent peaks of silicon, carbon and oxygen transitions while only weak signals are present for sulfur and molybdenum. The peak at 83 eV is characteristic of silicon suboxide, SiO_x ($x < 2$) which lies between metallic silicon and SiO₂ respectively at 92 and 78 eV [4, 18]. SiO_x appears as a consequence of the reaction between the container (quartz tube) and the sample resulting in the formation of pseudo-ternary PbMo₆S_{8-x}O_x. This is well supported by XRD data [4, 19]. Additional evidence for the SiO_x phase was obtained from EDX analysis (Fig. 1). It was, however, impossible to distinguish and quantify the oxygen content of PbMo₆S_{8-x}O_x and SiO_x by AES, even after prolonged sputtering, as the latter diffuses very rapidly and covers completely the surface (Fig. 2) in contrast to the deliberately oxygenated samples [4].

A fairly large carbon peak was observed on the fractured surface of the oxygen contaminated sample. This is due to hydrocarbon contamination [17], typically detected on the air-exposed samples, as these samples were handled in air prior to Auger measurements. However, it is interesting to note that upon sputtering, the carbon peak diminishes along with silicon and oxygen peaks. Nevertheless, they reappear and gradually grow with time. In fact, the spectrum recorded after an hour of sputtering closely resembles that of the fractured one indicating interdiffusion of the impurities. This evolution is represented in Fig. 2. A similar trend is observed even after prolonged sputtering. However, very little carbon is detected on the samples prepared by the methods I and II. This can be correlated to the relative porosity of the samples which is in accordance with the SEM results (Fig. 3). Density measurements further support this idea. For example, the oxygenated sample has a density of about 80% of the theoretical value while the others have much higher densities (95% or above), see Table 1.

Irrespective of the method of preparation, the surface compositions (S/Mo ratio) estimated from the fractured and sputtered specimens are respectively in the range 2.5 ± 0.2 and 1.25 ± 0.1 . The observed sulfur enrichment on the fractured surface of PbMo₆S₈, compared to the ideal composition; S/Mo ratio = 1.33 (ca. 8/6), indicate a quite different behavior at the interface. As indicated earlier, this deviation from the stoichiometric value is due to the presence of sulfur excess phases at the grain-boundaries. Unlike the carbon and SiO_x, there is no observable diffusion/segregation of the constituent elements, namely lead, sulfur and molybdenum. A representative example is shown in Fig. 4.

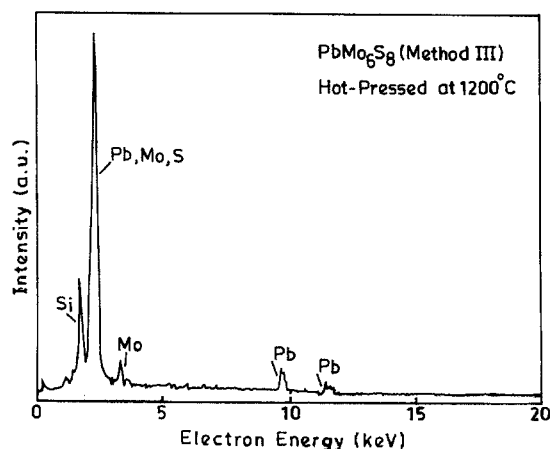


Fig. 1. EDX analysis of the sample prepared in a quartz tube

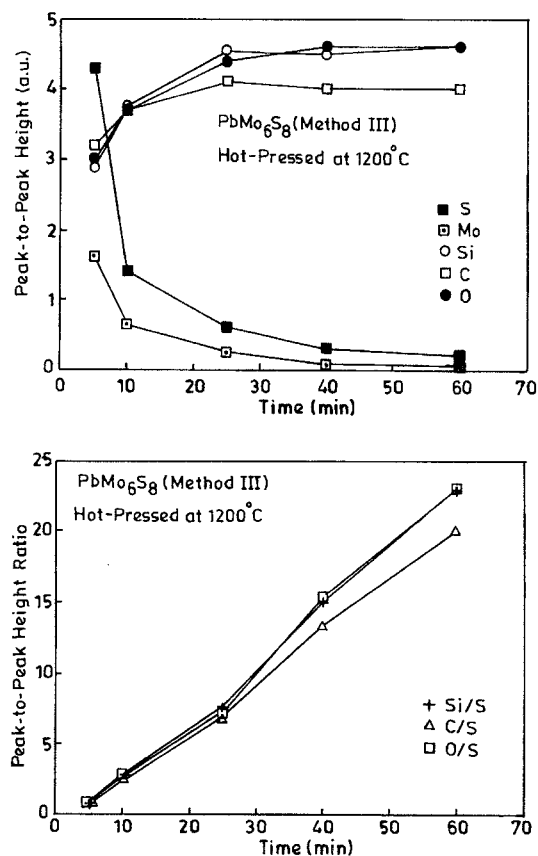
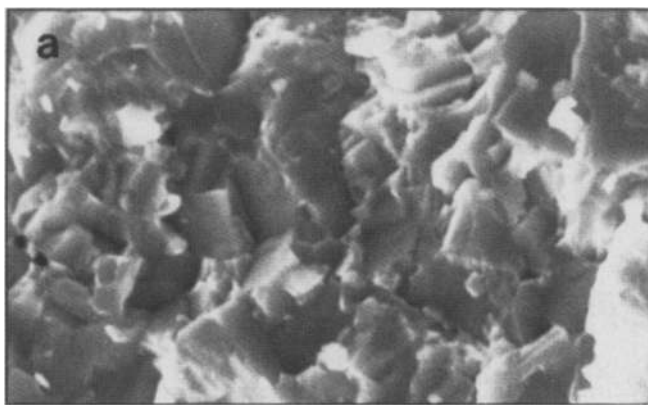


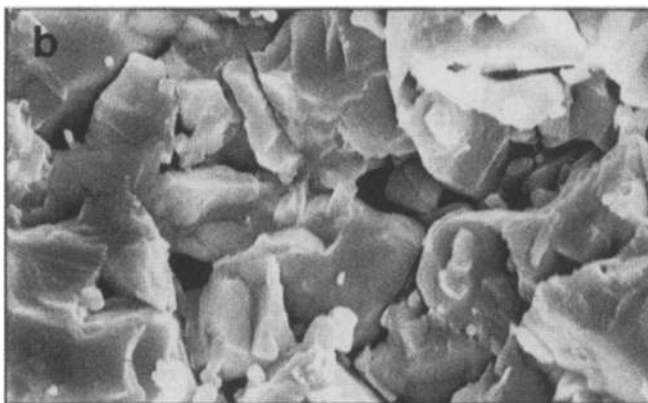
Fig. 2. Diffusion of impurities at the grain boundaries of sputtered (100 Å) sample

2.1 Effect of hot-pressing temperature

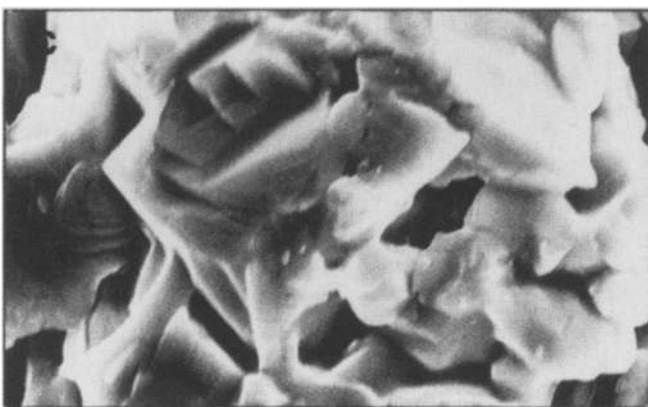
In terms of production of a smaller grain size and a favorable synthesis condition (1180°C for 2 h) of PbMo₆S₈, method I emerges as promising (Table 1). Hence, these samples were further studied in detail with respect to varying hot-pressing temperatures (1000–1400°C) at a constant pressure of 2 kbar for 1 h. This was done to optimize the processing temperature so as to achieve a higher density and better intergrain connection.



Method I 5 μm



Method II 5 μm



Method III 5 μm

Fig. 3a-c. SEM of PbMo_6S_8 prepared by different methods. All the samples were hot-pressed at 1200°C

The measured densities of the samples hot-pressed at three different temperatures, viz 1000, 1100 and 1200°C , are respectively 70, 80, and 95%. As expected a significant amount of carbon is observed on the fractured surface. The high porosity of the samples allow the atmosphere to percolate through and provides a means by which a large

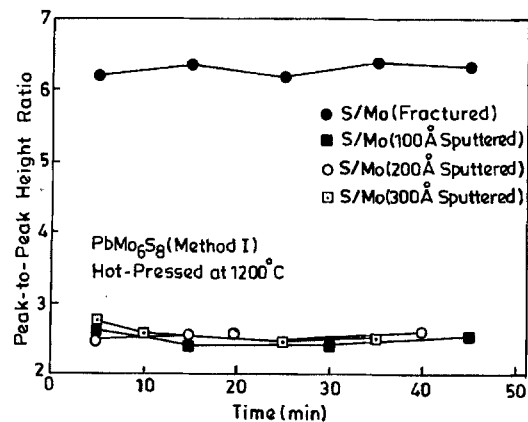
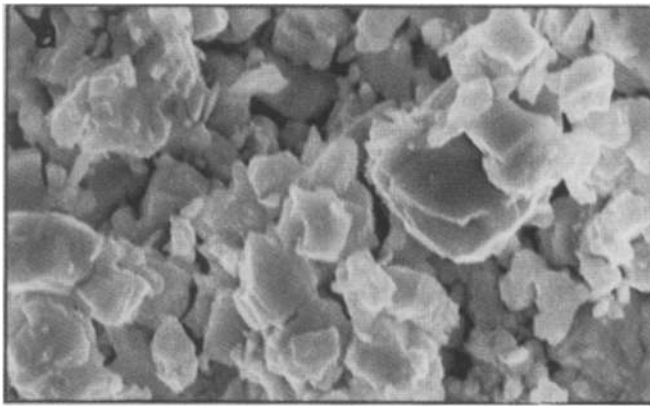


Fig. 4. Auger elemental composition ratios of one of the samples

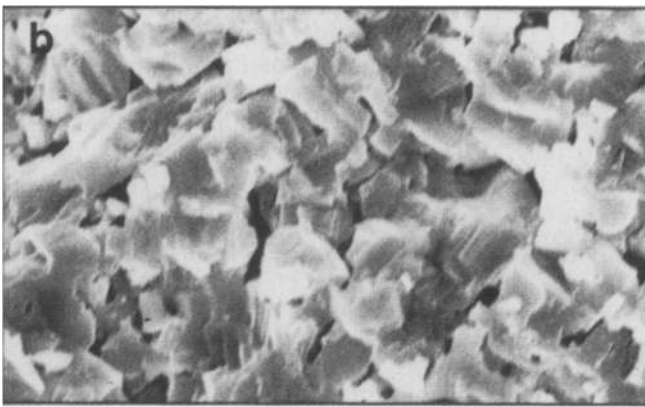
amount of hydrocarbons is entrapped and is best supported by the micrograph (Fig. 5a). The huge carbon peak, however, was reduced in magnitude to a considerable extent by sputtering. Nevertheless, after one hour, it has saturated once again regaining the original carbon signal amplitude, in an identical fashion to Fig. 2.

On the high density samples (hot-pressed $\geq 1200^\circ\text{C}$) the carbon signal is greatly reduced or nearly absent. The pores are considerably diminished due to better intergrain connections (Fig. 5c). It is interesting to note that the samples hot-pressed under identical conditions, at 1200°C , but prepared by different methods, show somewhat different behavior towards carbon contamination. This can be related to their distinct microstructures as shown in Fig. 3. For example, in the coarser-grained samples (methods II and III; 5–10 μm), a considerable amount of carbon is detected at a few sites immediately after fracture in contrast to the fine-grained sample (method I; 0.5–2.0 μm) where most of the areas are free of carbon. Significant numbers of voids and pores are expected due to a poor densification of larger grained samples. This suggests that PbMo_6S_8 is highly susceptible to atmospheric contamination and is in agreement with the earlier suggestion of carbon-induced degradation of J_C [20].

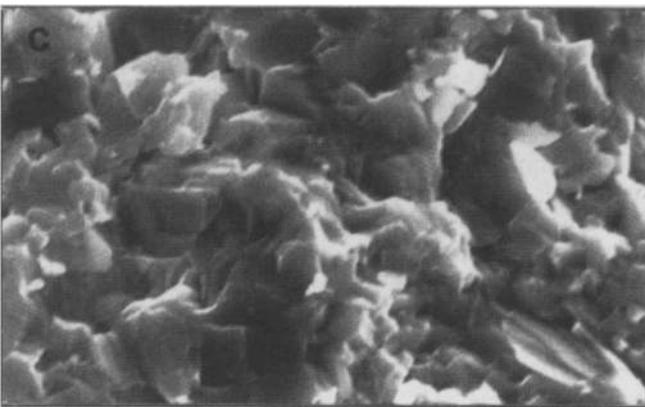
Interestingly, there seems to be a notable change in the S/Mo ratios with the increase of hot-pressing temperature. As can be seen from Table 2, a variation of surface concentration, on both fractured and sputtered surfaces, is evident. This may well be manifested in a possible initiation of the alteration of the ternary composition in association with precipitation of MoS_2 at higher temperatures [21]. That is, the heat treatment in vacuum at higher temperatures causes a certain amount of degradation of the material and becomes pronounced over a period of time, as in the case of a sample processed at 1250°C . This resulted in progressive broadening and reduction of the amplitude of the specific heat jumps and therefore the observed T_C distribution (Fig. 6). The smearing of the sharp distribution of T_C suggest that a composition variation, a plausible non-stoichiometry, is likely in the near-surface regions. Two other possible reasons for this observation, namely (i) incomplete reaction [10], and (ii) oxygen contamination [4] can be discarded by considering the fact that the samples used in the present investigation



HP - 1000°C ─────────── 5 μm



HP - 1100°C ─────────── 5 μm



HP - 1200°C ─────────── 5 μm

Fig. 5a-c. SEM of PbMo_6S_8 hot-pressed (HP) at different temperatures. The sample was prepared by method I

are highly crystalline and oxygen free. The atomic concentration profile ratio (S/Mo) for one of the samples hot-pressed at 1200°C is displayed in Fig. 7. After the initial variation in the S/Mo ratio, it attains a steady state around 75–100 Å corresponding to the bulk composition.

Table 2. Auger elemental concentration ratios of the hot-pressed PbMo_6S_8 samples prepared by method (I)

| Hot-pressing temperature (°C at 2 kbar for 1 h) | Sulfur/molybdenum ratio ^a | |
|--|--------------------------------------|-------------------|
| | In situ fractured | Sputtered (100 Å) |
| 1000 | 2.58 (4) | 1.31 (3) |
| 1100 | 2.65 (5) | 1.26 (2) |
| 1200 | 2.60 (5) | 1.20 (3) |
| 1250 ^b | 2.68 (4) | 1.15 (4) |
| 1300 | 2.66 (4) | 1.16 (3) |
| 1400 | 2.74 (4) | 1.13 (4) |

^a Ideal value is $8/6 = 1.33$

^b For 2 h

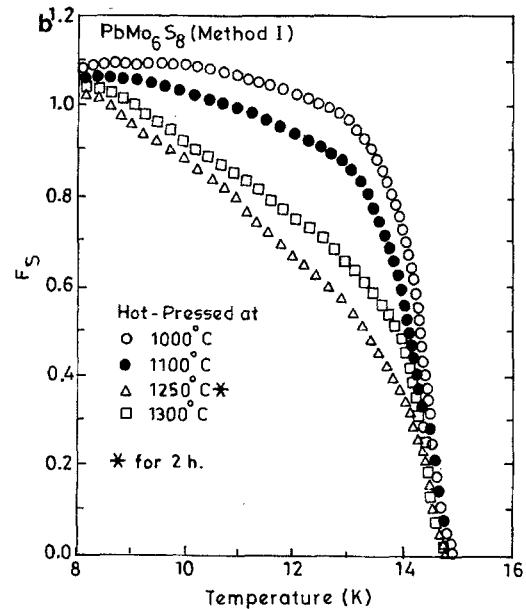
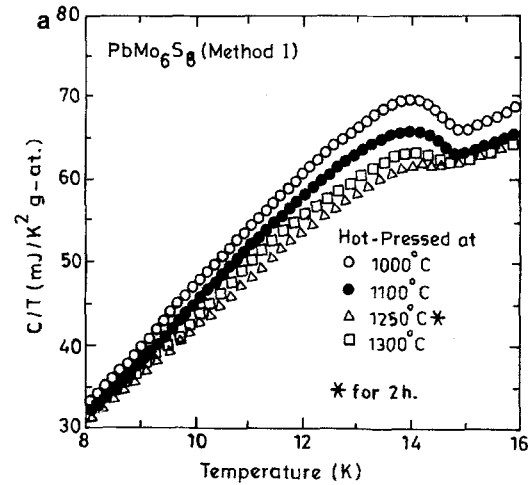


Fig. 6a, b. The specific heat jump (a), and the T_C distribution (b) of hot-pressed samples

However, the extrapolation of this behavior to the surface leads to a S/Mo ratio very close to the ideal value. As suggested earlier, the slightly lower values of the S/Mo ratio are due to preferential sputtering of sulfur. It should

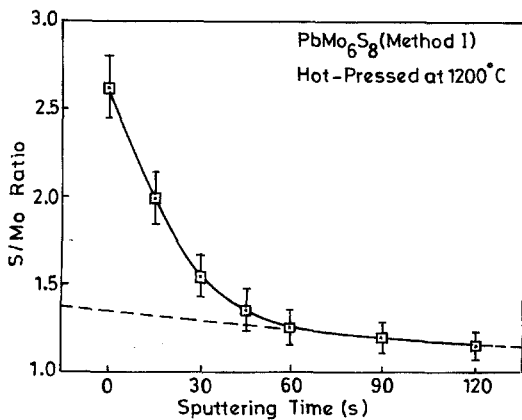


Fig. 7. Auger depth profiles of one of the samples

be noted here that the grain-boundary phases extends over 200 Å depth for some of the samples.

2.2 Critical current limitations

Well connected grains or high density samples are the essential prerequisite for a reasonable J_C . On the porous samples the current flows percolatively and there is thus a reduction in the measured J_C values. As shown in Table 1 and Fig. 3, large grained samples achieve a maximum density of only about 94% compared with the smaller grained samples that can nearly be compacted to the theoretical density. Close to T_C , interpretation of the ac-susceptibility data is consistent with a granular behavior. The grain-boundary phases, as well as many of the finely distributed—as yet unidentified—defects at the interface would usually be beneficial by serving as flux-pinning centers. Because of the thicker grain boundaries (of the order of 100–200 Å), compared to the coherence length (28 Å) of PbMo_6S_8 [22], they instead play the role of weak-links with a devastating effect on the critical current. However, they can greatly be reduced by incorporation of appropriate elements which stabilize the ternary PbMo_6S_8 phase. This turns out to be an effective way to improve the intergrain connection [23] and a successful approach in minimizing the grain-boundary thickness with the simultaneous benefit of achieving excellent homogeneity [24].

The failure to achieve the expected large critical current densities of PbMo_6S_8 are partly due to the coexistence of various amounts of triclinic and rhombohedral phases [6–8]. Such a phase transformation is known to occur in $M\text{Mo}_6\text{S}_8$ ($M = \text{Eu}, \text{Ba}, \text{Sr}, \text{Ca}$) and suppress superconductivity [25]. The low-temperature triclinic fraction, however, strongly depends on the grain sizes of PbMo_6S_8 , i.e., the smaller the grain, the lesser the transformation [8]. While granularity, grain-boundary phases, and phase transition all contribute to the weak-link behavior, one another factor, namely the inhomogeneities in PbMo_6S_8 may also be equally important. A small change in the ternary composition may be associated with suppression or loss of superconductivity. The appreciable width in the calorimetric transitions can be accounted by

considering the possible non-stoichiometric composition for both sulfur and lead defects in $\text{Pb}_x\text{Mo}_6\text{S}_{8-y}$. However, such a compositional dependence has not been determined clearly as yet. The possibility of sulfur deficiency was, however, checked by synthesizing homogeneous single-phase samples in a thermo-sealed boron nitride crucible. Independent of the initial sulfur concentration ($\text{Pb}_1\text{Mo}_6\text{S}_{8-y}$; $y = 0.0-0.8$), T_C is found to be optimal (14.5–14.8 K). Furthermore, there is a strong correlation between the initial sulfur concentration and the lead or molybdenum impurities in the final product [10, 15]. In contrast, a narrow homogeneity range of $\text{Pb}_x\text{Mo}_6\text{S}_{8-y}$ ($x = 0.95-1.05$; $y = 0.2-0.45$) was reported with a T_C values of 8–15 K [26]. Although it is tempting to relate this observation to our T_C distribution, it should be noted that such samples were prepared in quartz tubes. Therefore, one has to make sure that they are free from a possible oxygen contamination, which is usually the case [4], before making any comments. However, independently of the exact mechanism of the non-stoichiometry, the possible occurrence of inhomogeneities in the samples at the grain-boundaries affects the T_C . This means that such non-stoichiometric phases may have a lower critical field, B_{t2} , [10, 15] and hence lower J_C .

3 Conclusion

The accumulated impurities, such as carbon, and SiO_x (in one of the series), in the voids of the fractured PbMo_6S_8 diffuse rapidly to surface. The former arises as a result of atmospheric contamination, and the latter is as a consequence of reaction with the quartz tube used for the preparation of some of these compounds. This further induces the formation of the undesired $\text{PbMo}_6\text{S}_{8-x}\text{O}_x$ phase which is known to possess lower T_C and H_{c2} values and hence J_C . Segregation of significant amounts of sulfur-rich binary phases, such as MoS_2 , Mo_2S_3 and PbS were found at the interface. They extend up to a depth of 75–100 Å or more and act as a barrier to the current flow. Yet another problem is the inhomogeneity within the samples resulting in a smearing of T_C down to 9 K and this is due to the formation of a continuous non-stoichiometric phase in the near-surface region. Even a subtle compositional inhomogeneity at the grain-boundary would certainly influence the electronic structure. Thus, in PbMo_6S_8 , the presence of impurities, secondary phases, and the inhomogeneity with respect to the ternary composition, are sufficient to limit the electron transfer across the boundaries. Hence, they stand as a likely contributor to the problems of low critical current densities in these materials in addition to the problems of granularity and phase transition.

Acknowledgements. This work is supported by the Commission (Suisse) pour l'Encouragement de la Recherche Scientifique (CERS) within EUREKA'96. We thank Dr. D. Cattani and Dr. Ph. Niedermann for their keen interest and useful discussions; Mr. S. Ritter and Mr. A. Stettler for the technical assistance.

References

1. *Proc. Int'l Workshop on Chevrel-Phase Superconductors*, Hôtel de Chavanne-de-Bogis, Switzerland (1991) pp. 1–79
2. Ø. Fischer, B. Maple (eds.): *Superconductivity in Ternary Compounds I, II*, Topics Curr. Phys. Vols. 32, 34 (Springer, Berlin, Heidelberg 1982)
3. See for example: L. Le Lay, T.C. Willis, D.C. Larbalestier: *Appl. Phys. Lett.* **60**, 775 (1992);
D. Cattani, J. Cors, M. Decroux, Ø. Fischer: *IEEE TM-27*, 950 (1991);
H. Yamasaki, M. Umeda, Y. Kimura, S. Kosaka: *IEEE TM-27*, 1112 (1991);
G. Rimikis, W. Goldaker, W. Specking, R. Flükiger: *IEEE TM-27*, 1116 (1991)
D.W. Capone II, D.G. Hinks, D.L. Brewster: *J. Appl. Phys.* **67**, 3043 (1990)
L. Le Lay, P. Rabiller, R. Chevrel, M. Sergent, T. Verhaege, J.C. Vallier, P. Genevey: *Adv. Cryog. Eng.* **36**, 3298 (1990)
M.O. Rickel, T.G. Togonidze, V.I. Tsebro: *Sov. Phys.-Solid State* **28**, 1496 (1986)
4. P. Selvam, D. Cattani, J. Cors, M. Decroux, A. Junod, Ph. Niedermann, S. Ritter, Ø. Fischer, P. Rabiller, R. Chevrel, L. Burel, M. Sergent: *Mater. Res. Bull.* **26**, 1211 (1991)
5. P. Selvam, D. Cattani, J. Cors, M. Decroux, A. Junod Ph. Niedermann, S. Ritter, Ø. Fischer, P. Rabiller, R. Chevrel: *J. Appl. Phys.* **72**, 4232 (1992)
6. J.D. Jorgensen, D.G. Hinks: *Solid State Commun.* **53**, 289 (1985)
J.D. Jorgensen, D.G. Hinks, G.P. Felcher: *Phys. Rev. B* **35**, 5365 (1987)
7. C. Meingast, W. Goldacker, U. Wildgruber: In [1] p. 7
8. M. Francois, K. Yvon, D. Cattani and M. Decroux, R. Chevrel, M. Sergent, S. Boudjada, Th. Wroblewski: *J. Appl. Phys.* **75**, 423 (1994)
9. P. Selvam, D. Cattani, J. Cors, M. Decroux, Ph. Niedermann, Ø. Fischer: In [1] p. 31
10. M. Decroux, P. Selvam, J. Cors, B. Seeber, Ø. Fischer, P. Rabiller, R. Chevrel: *IEEE Trans. AS-3*, 1502 (1993)
11. M. Decroux, D. Cattani, J. Cors, S. Ritter, Ø. Fischer: *Physica B* **165&166**, 1395 (1990)
12. R.W. Rollins, H. Kupfer, Z.W. Gey: *J. Appl. Phys.* **45**, 5392 (1974)
13. D. Cattani: Etude des densités de courant critique dans le composé PbMo_6S_8 . Dissertation no. 2422, Université de Genève (1990)
14. L.E. Davis, N.C. MacDonald, P.W. Palmberg, G.E. Riach R.E. Weber (eds.): *Handbook of Auger Electron Spectroscopy* (Physical Electronics, Eden Prairie, MN 1976)
15. J. Cors: Propriétés superconductrices sous champ magnétique du composé PbMo_6S_8 étudiées par chaleur spécifique. Dissertation no. 2456, Université de Genève (1990)
16. A. Junod, T. Jarlborg, J. Muller: *Phys. Rev. B* **27**, 1568 (1983)
17. D. Briggs, M.P. Seah (eds.): *Practical Surface Analysis*, 2nd edn., Vol. 1 (Wiley, Chichester 1990)
18. J. Derrien, M. Commandre: *Surf. Sci.* **118**, 32 (1982)
19. D.G. Hinks, J.D. Jorgensen, H.-C. Li: *Phys. Rev. B* **51**, 1911 (1983)
20. W. Goldaker, E. Seibt, G. Rimikis, R. Flukiger: In *Proc. 2nd Int'l Conf. on Modern Superconductivity towards Applications* (IITT-Int'l, Paris 1990) p. 99
21. P. Selvam, D. Cattani, J. Cors, M. Decroux, Ph. Niedermann, S. Ritter, Ø. Fischer, L. Burel, R. Chevrel, P. Rabiller, M. Sergent: In *Proc. 3rd Int'l Conf. on Superconductivity — Materials, Physics and Applications* (IITT-Int'l, Paris 1991) p. 157.
22. G.L. Dorofejev, E.Y. Klimenko, S.V. Frolov, E.V. Nikulenkov, E.I. Plashkin, V.Y. Filkin: In *Proc. MT-9*, Zurich, (1982) p. 564
23. P. Selvam, D. Cattani, J. Cors, M. Decroux, Ph. Niedermann, Ø. Fischer, R. Chevrel, T. Pech: *IEEE Trans. AS-3*, 1575(1993)
24. P. Selvam, J. Cors, D. Cattani, M. Decroux, Ø. Fischer, E.W. Seibt: *Appl. Phys. A* (submitted)
25. R. Baillif, A. Dunand, J. Muller, K. Yvon: *Phys. Rev. B* **47**, 672 (1981)
R. Baillif, A. Junod, B. Lachal, J. Muller, K. Yvon: *Solid State Commun.* **40**, 603 (1981)
B. Lachal, R. Baillif, A. Junod, J. Muller: *Solid State Commun.* **45**, 849 (1983)
26. S. Yamamoto, M. Wakihara, M. Taniguchi: *Mater. Res. Bull.* **20** 1493 (1985)